Is tropospheric ducting a myth?

Mike Hasselbeck, WB2FKO

mph@sportscliche.com

Revision date: 26 May 2025

Abstract

Radio wave propagation in the troposphere is analyzed using a ray-trace approach. When the refractive index of air decreases as a function of altitude, which is the usual situation, ray paths may be slightly bent. This refraction gradient, however, is insufficient to form an effective communication duct. Temperature inversions are often claimed to create an abrupt boundary between air layers that can trap radio waves, but the angles required are too shallow for communication between realistic amateur VHF installations. Low-altitude tropospheric forward scattering from the turbulent mixing of warm and cool air accompanying an inversion is proposed as an alternative explanation to ducting.

Keywords: propagation, troposphere, refraction, reflection, scatter, ducting

Introduction

Understanding how radio waves propagate in the troposphere is essential for the successful implementation of radar systems [1, 2]. Echoes from targets located beyond line-of-sight have been observed since the early days of radar and motivated efforts to identify the physical causes. Unlike the ionosphere, the troposphere has an insufficient density of free charges – electrons and ions – to affect the propagation of radio waves. Reflection, diffraction, and primarily refraction by air masses were postulated as possible mechanisms and led to the first descriptive models [3]. We distinguish between the detection of radar reflections from airborne objects by a single transmitter-receiver and instead focus on point-to-point communication between two stations located at a separation distance beyond their horizons.

Our present understanding of DX propagation in the troposphere involves two distinctly different phenomena: scattering and ducting. They are primarily relevant for VHF+ frequencies. Scattering can occur at any altitude up to about 15 km and is always present, although it is characterized by very weak signals. Ducting, on the other hand, is a relatively rare occurrence that has been linked to cyclonic weather patterns. Two-way communication over thousands of kilometers can occur with paths over water being the most effective [4, 5].

There are two models of tropospheric ducting that are based on refraction occurring in air. The first invokes the altitude dependence of the refractive index that is known to bend the path of radar beams. The second asserts the presence of a waveguide-like channel formed between the troposphere and earth (surface duct) or entirely between layers in the troposphere (elevated duct). A waveguide picture is attractive because it explains the extreme distances that can be attained as well as the observed wavelength dependence: ducting is more prevalent at UHF and microwave, much less common at VHF, and unknown at lower frequencies. Openings can last for hours and sometimes days [6].

We will show that neither of these physical pictures are tenable. The primary issue is that although the refractive index of air changes as a function of pressure, temperature, and humidity, the variations are so small that they minimally affect the ray path. Refraction is important for radar applications but is inconsistent with the geometry required for communication between ground-based VHF stations having realistic antenna takeoff angles. The waveguide interpretation requires an almost perfectly smooth interface between air layers to induce any appreciable reflection and this must be maintained over enormous distances. Because the refractive index is independent of radio frequency, the proposed duct is claimed to have a cutoff wavelength that prevents sufficiently low frequencies from propagating through it. Cutoff happens when the waveguide cross section is of the order of a wavelength, suggesting a stable channel of less than 1 meter width that extends over 1000 km. It is hard to understand how such a structure could exist and persist in a dynamic atmosphere.

This paper analyzes radio communication via tropospheric refraction using the principles of physical optics. We identify the limitations imposed by realistic index gradients followed by a critical examination of ducting caused by inversion layers. The possibility of beam bending by lens-shaped air masses is also considered. Low-altitude tropospheric forward scattering is proposed as a more plausible explanation for the long-haul communication paths that coincide with weather fronts.

Vertical Stratification and Ray Tracing

Snell's Law quantifies the angle at which electromagnetic radiation is bent or refracted as it traverses different media. Referring to Fig. 1 (left), a light ray or radio wave propagating in a medium with refractive index n_1 encounters a medium with index n_2. The angles of incidence θ_1 and refraction θ_2 are defined with respect to the surface normal depicted by the dashed vertical line. The refracted ray is deflected at an angle as determined by the following equation [7]:

$$n_1 \sin\theta_1 = n_2 \sin\theta_2 \tag{1}$$

This is valid for any arbitrary geometry such as a spherical surface shown in Fig. 1 (right). The surface normal in this case is the radius of curvature; glass and plastic lenses are readily analyzed this way.

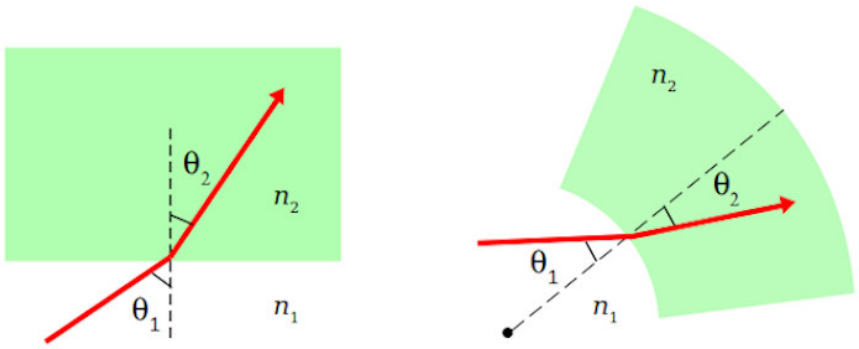

Figure 1: Ray refraction for two different surface geometries. When $n_2 > n_1$, the refracted ray is bent towards the surface normal.

The troposphere is the lowest layer of the atmosphere and is composed of air that may be at different pressure, temperature, or humidity. Variation of these parameters causes the refractive index of air to change with altitude; these changes are only on the order of 1 part in 10^4. This is in strong contrast to the ionosphere, where the refractive index is described by plasma physics. The ionosphere presents distinct index differences and Fresnel surfaces that can completely reflect a radio wave over a wide range of incidence angles. Ionization in the troposphere is negligible.

Measurements have shown that in standard conditions in the lower troposphere the index decreases at an approximately linear rate (γ) as a function of altitude (h) [8]:

$$n(h) = n_0 + \gamma h \tag{2}$$

where n_0 is the refractive index at ground level ($h = 0$). The index of air is just above unity, with nominal values of $n_0 = 1.00035$ and $\gamma = -39 \times 10^{-6}$ km^{-1}. It is also known to have negligible dispersion at radio frequencies, i.e. ray tracing will behave the same for a wide range of wavelengths [9].

It is important to emphasize that the index of pure vacuum is identically 1. For $h \geq (1 - n_0)/\gamma$, Eq. (2) predicts that the refractive index of the troposphere will be less than 1 or even negative, which is not physical. Correct use of this equation must respect this limit, i.e. we must always have $n(h) \geq 1$ [8].

The existence of an index gradient can cause a radio wave that is launched at ground level into the troposphere to have a curved trajectory. Possible paths are sketched in Fig. 2. When the index remains constant ($\gamma = 0$), the ray is unaffected and propagates in a straight line above the horizon (Path A). With $\gamma < 0$, the trajectory curves toward the earth's surface (Path B). This is known as *super-refraction*. When γ is sufficiently negative, the ray is said to be trapped (Path C) and returns to the surface. There may be multiple hops from ground reflections to the trapping layer, leading to the concept of a *duct* that can enable extended communication paths, well beyond line-of-sight.

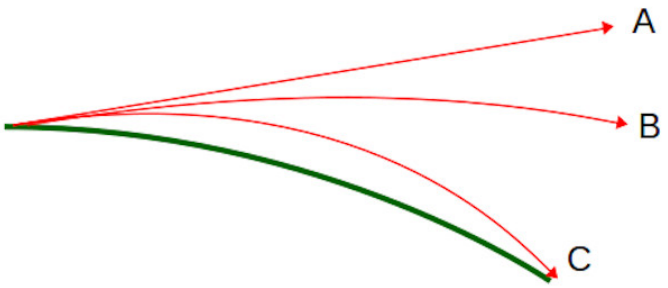

Figure 2: Different ray trajectories in the troposphere. Path A: No refraction ($\gamma = 0$). Path B: Super-refraction causes the ray to curve downwards. Path C: Trapping returns the ray back to the surface.

For a wave launched horizontally at zero degrees elevation, Appendix A shows that an index gradient of $\gamma = -156.8 \times 10^{-6}$ km^{-1} will cause the ray to propagate parallel to the earth's curvature [1, 2, 8]. This is the starting point for the analysis, which must include ray trajectories above horizontal over a range of angles.

It is frequently asserted that trapping is caused by a wave refracting back to the earth's surface. For vertically stratified layers, Appendix B demonstrates that refraction alone cannot accomplish this. The trigonometric constraints imposed by Snell's Law prevent any refraction at angles beyond

90 degrees from surface normal. This is the case in both planar and curved layers. Trapping results not from refraction, but from *total internal reflection* of rays that are incident at grazing angles to the index gradient. We follow the methodology of Zeng *et al* where the key role of total internal reflection to produce trapping has been emphasized [8].

A realistic model of propagation in the troposphere should include a range of antenna takeoff angles $\alpha_0 > 0$ degrees. When accounting for ground reflection, even a high-performance amateur VHF station with antenna pointed at the horizon will have the main radiation lobe at an elevation angle in excess of 3 degrees. For the troposphere to attain total internal reflection and trapping at non-zero takeoff angles, the index gradient γ must decrease (become more negative) to compensate. This can be calculated directly using Eq. (B.13); results are shown in Fig. 3.

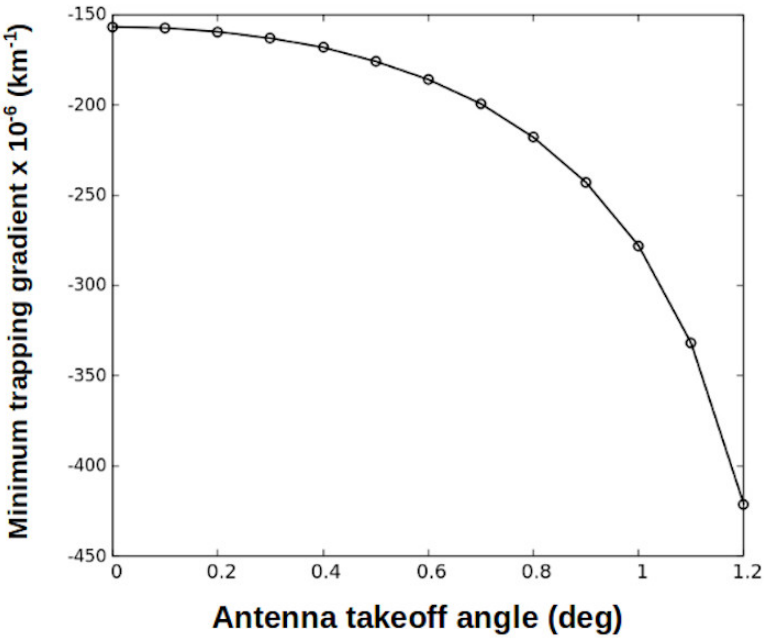

Figure 3: Minimum vertical index gradient (γ) to trap a ray for different takeoff angles.

The calculation uses index $n_0 = 1.00035$ at ground level with a linear decrease given by Eq. (2). A takeoff angle that is only one degree above horizontal requires a substantial decrease of the index gradient to trap the wave. This is explained by the lower altitude at which $n(h) = 1$ is reached with steeper gradients. Because the index cannot go below unity, any ray reaching this point without reflecting will escape from the troposphere. When the wave is launched horizontally, this critical altitude is 2.14 km; it drops to 831 meters when the takeoff angle is 1.2 degrees. The needed index gradient at this angle is more than 10 times the generally accepted value for normal atmospheric conditions.

Additional insight is obtained by fixing the index gradient and tracing ray paths at different takeoff angles. In Fig. 4, γ is set to -332×10^{-6} km^{-1}; this is the minimum needed to trap a ray at a takeoff angle of 1.1 degrees. Note that the propagation distance is along the curved surface of the earth. The relatively large negative index gradient causes the ray launched at 0.5 degrees to be trapped at an altitude of 217 meters and return to the earth at a distance 99 km from the takeoff point. The 1.1 degree ray reaches an altitude of 1.05 km where it is reflected to a point 212 km from the source. The gradient is insufficient to trap the ray launched at 1.2 degrees and it escapes. While refraction produces the curved paths shown in Fig. 4, it must be emphasized that it is total

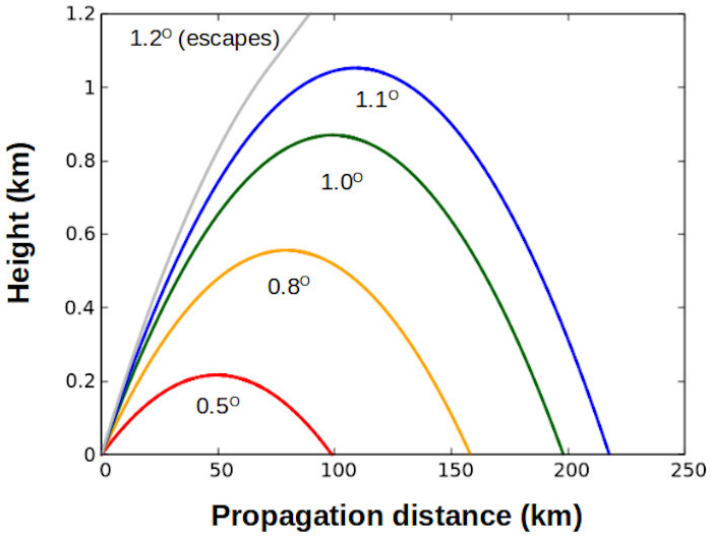

Figure 4: Calculated ray paths for takeoff angles α_0 in a range between 0.5 and 1.2 degrees. The index gradient $\gamma = -332 \times 10^{-6}$ km^{-1}. Rays with initial trajectories $\alpha_0 \geq 1.2°$ escape from the troposphere.

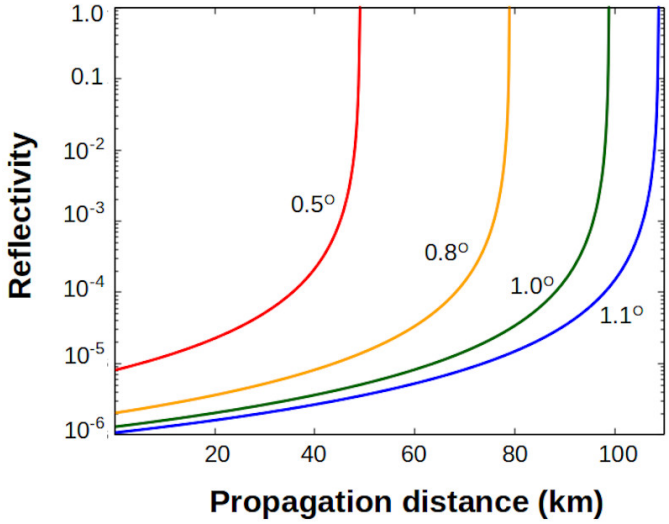

Figure 5: Calculated reflectivity at each point along the path for the rays shown in Fig. 4.

internal reflection at peak altitude that causes the rays to return to the surface.

The reflectivity experienced by the rays depicted in Fig. 4 changes as a function of altitude. Figure 5 plots the Fresnel reflection coefficient for horizontally polarized waves as given by Eq. (B.14). In each case, reflectivity is negligibly small until it increases abruptly; it resembles a step-function (note the log scale). This happens because the total internal reflection condition is being approached with grazing angles while the index is dropping continuously. This should be contrasted to the behavior of the ionosphere above the critical density, which acts as a reflecting surface for all angles of incidence at the same height, i.e. like a mirror.

This model of the troposphere shows that it is an inefficient reflector of radio waves launched at ground level and not conducive to propagation by ducting. Robust and reliable reflections – such as as occur in a waveguide or optical fiber – are not present. In the troposphere, reflectivity is

extremely sensitive to altitude, angle of incidence, and index gradient. This picture of trapping is inconsistent with expected antenna takeoff angles having a corresponding 3-dB primary lobe width of many degrees. Fig. 4 demonstrates that even in steep index gradients producing strong refraction, most of the incident radiation lobe is lost; the remaining low-angle rays will be reflected incoherently to widely separated points on the surface. High-gain antennas placed at heights well above ground obstacles offer only marginal improvement. Lack of any substantial reflectivity below the trapping altitude removes the possibility of interference or duct formation *within* the troposphere. These general conclusions still hold if the gradient is present in a channel located above the surface, i.e. no elevated ducting can be reasonably expected.

Inversions

An inversion may occur, for example, when warm air overruns a cooler layer. Instead of an index gradient, an abrupt boundary is established that separates two media with distinguishable indices of refraction. The model for a single spherical interface described by Eqs. (B.15)–(B.18) in Appendix B is used to calculate the reflectivity. A simple curved boundary is useful to illustrate the consequences of a small index difference across an interface.

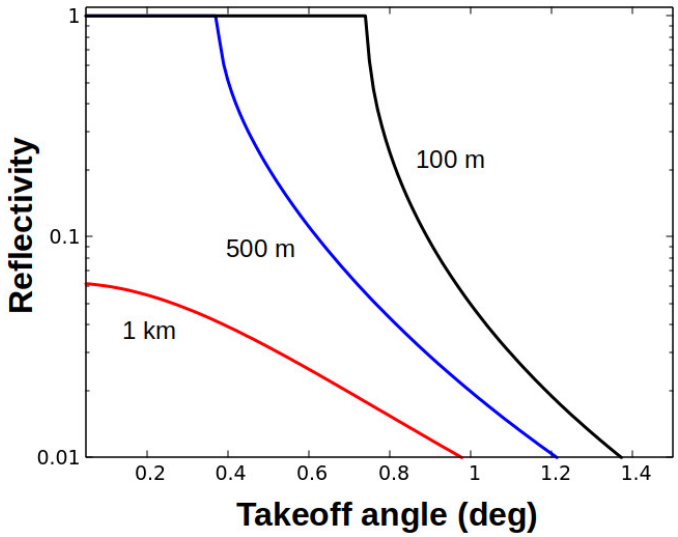

Figure 6: Calculated reflectivity (Γ) at the boundary between warm and cold air masses at three different altitudes as a function of antenna takeoff angle.

In the absence of an index gradient, a ray leaving the antenna at takeoff angle α_0 travels in a straight line until it meets the warm-cold boundary at height h. Values for the two indices can be obtained from the ducting profiles found in Ref. [8]. A larger difference between n_0 and n_1 leads to a more effective reflecting surface. We take optimal values of $n_0 = 1.00035$ for the cool lower layer and $n_1 = 1.00025$ for the warm air above it and calculate the reflectivity for horizontal polarization as a function of α_0. Results are shown in Fig. 6 for boundaries located at $h = 100$, 500, and 1000 meters.

The curves in Fig. 6 demonstrate that the interface can behave as an efficient reflecting surface, but only for warm air close to the ground at takeoff angles that are nearly horizontal ($\alpha_0 < 1$ degree) [10, 11]. Total internal reflection occurs when Eq. (B.17) produces $\Gamma = 1$. The behavior is

similar to the calculations in the previous section; the root cause is shallow angles and small index discontinuities at the layer boundary. Even a high performance antenna system will have most of its radiation lobe outside the angular range needed for reflection.

This conclusion is reinforced by calculating the sensitivity of reflected power to changes in the interface altitude h. Using the same indices n_0 and n_1 and an antenna takeoff angle of 0.5 degrees, Fig. 7 shows that all incident power is reflected for $h \leq 390$ meters. When the boundary height increases by just 30 meters, the reflected power drops by more than 3 dB. We further caution that the above calculations assume perfectly smooth surfaces. Real-world behavior will certainly be degraded compared to this mathematical idealization. Convective air currents will increase with the thermal gradient and quickly smear out the interface.

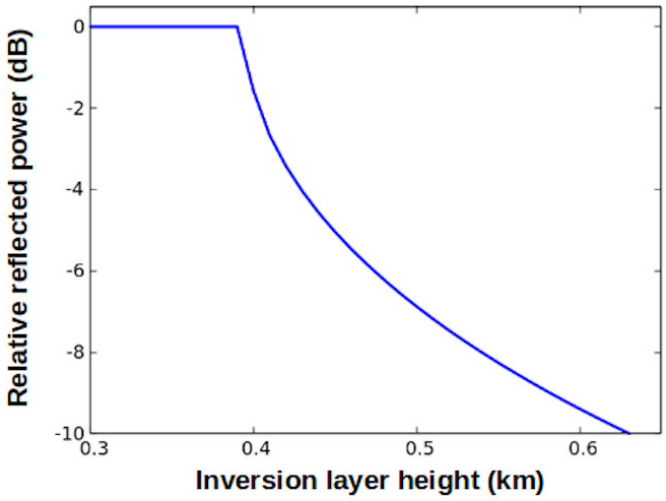

Figure 7: Calculated reflected power at an abrupt interface between warm and cold air masses located at different altitudes h for an antenna takeoff angle of 0.5 degrees.

The record-setting microwave contacts between California and Hawaii spanned a distance of 4024 km [5]. It has been postulated that the over-water propagation was enabled by an elevated duct with thickness on the order of 200 meters [11]. We can use Eq. (B.18) to estimate the number of hops required to cover the path. Assuming an ideal antenna takeoff angle of 0 degrees, a total of 40 hops are needed corresponding to 78 reflections. If any individual reflection point on either the upper or lower index boundary of the duct experiences a momentary disturbance on the scale of a wavelength, then the entire path will be disrupted. A propagation model involving such a large number of idealized reflections is highly implausible. It is also worth noting that if such a duct existed as described, it would enhance propagation on all HF amateur bands including 160 meters. There is, however, no evidence for this.

Horizontal Variations

When we allow for horizontal variation of the refractive index in the troposphere, prism- and lens-like structures can be considered. A prism or lens can arise from a pocket or blob of air with an internal index different than the air surrounding it. Examples are sketched in Fig. 8.

In the proper orientation, an air mass or sequence of air masses can potentially bend a radio wave

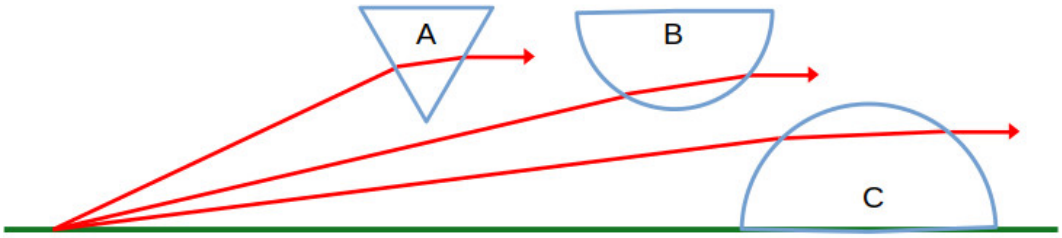

Figure 8: Ray tracing through various air masses having different internal and external refractive indices.

back to the surface entirely by refraction. An inverted prism is shown in Fig. 8(A). If the index is smaller inside the prism than outside, the ray is bent away from the surface normal and refracted at a larger angle. Upon exiting the prism, its trajectory is altered downward. This is opposite to what occurs with a glass prism in air. A spherical or cylindrical lens is shown at (B), where a smaller internal index bends the ray back toward the horizon. When the sphere is inverted as seen at (C), the ray will bend toward horizontal when its internal index is larger as in a conventional glass lens.

The extremely small internal-to-external refractive index variation ($\Delta n \approx 10^{-4}$) prevents these structures from refracting radio waves more than a few tenths of a degree. This means beam deflection is negligible making them entirely ineffective for ducting or coupling into a duct.

The combination of horizontal and vertical index variations in air suggests the concept of a graded-index cylindrical or ball lens as depicted in Fig. 9. The internal refractive index decreases linearly along a radial path r where Eq. (2) is rewritten:

$$n(r) = n_0 + \gamma r \tag{3}$$

In this geometry, the ray should become tangent to the index interface at some point on its trajectory and experience total reflection. This can be modeled numerically for different takeoff angles, radius of curvature, heights, and index gradients (γ). Analysis shows that ray paths that return to the surface as shown in Fig. 4 cannot be attained unless the radius tends to infinity, i.e. the circular shells approach planar layers [12]. Radii of many kilometers are unable to compensate for the very weak refraction between layers when γ is of the order 10^{-4} km^{-1}.

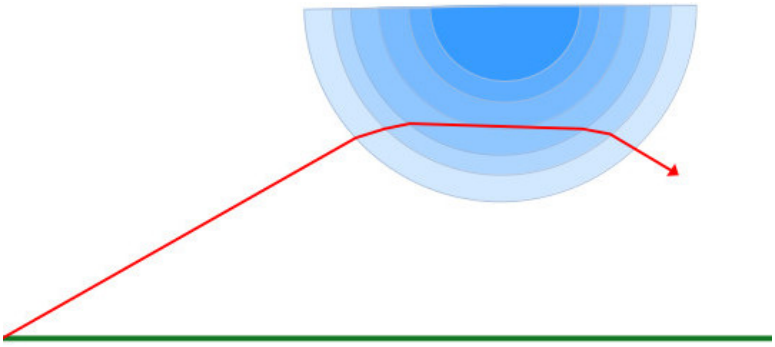

Figure 9: Spherical/cylindrical air mass with a radially varying internal index profile. The conceptual ray path shown in the sketch cannot be realized with index gradients found in the troposphere; it will traverse the air mass with very little deflection.

When surface curvature is coupled with minimal refraction, the ray cannot find a critical angle and will traverse the sphere without significant deflection. The same result is found when an index gradient is applied to the inverted hemisphere shown in Fig. 8(C). We conclude that refraction by thermal and/or humid air masses is ineffective for deflecting and propagating VHF signals over extended DX paths in the troposphere.

Tropospheric Scattering

Two well-equipped VHF+ stations can routinely communicate over DX paths approaching 700 km by means of tropospheric forward scattering. Anomalous weather conditions are not required. The source of this scattering is widely understood to be ongoing disturbances in the pressure-temperature-humidity profile of the turbulent upper-atmosphere. These air fluctuations have corresponding variations of refractive index that can scatter radio waves over a wide range of angles.

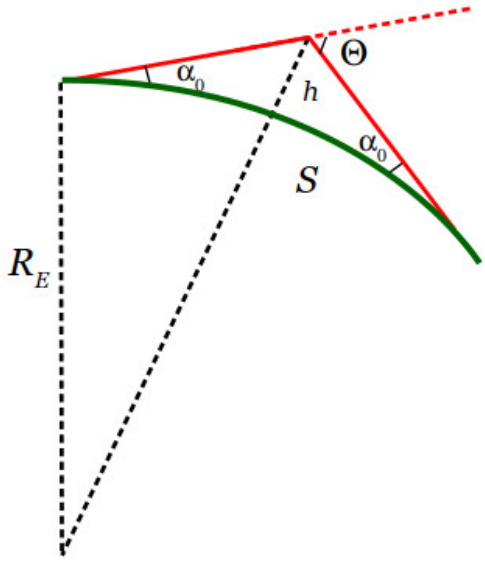

Figure 10: Geometry (not to scale) for calculating the DX path length (S) between two stations having identical antenna takeoff angles (α_0). The scattering volume is located at a height h above the surface.

Before considering the physical model for forward scattering, we can estimate the maximum DX path length given the geometric limits set by the maximum height of the troposphere (h), the radius of the earth (R_E), and antenna takeoff angles (α_0). The geometry is sketched in Fig. 10. For mathematical convenience, the two takeoff angles are taken to be identical and there is no index gradient, i.e. $\gamma = 0$. Using the Law of Sines, the path length S along the surface is:

$$S = 2R_E \left(\frac{\pi}{2} - \alpha_0 - \sin^{-1} \left[\frac{R_E}{R_E + h} \sin \left(\frac{\pi}{2} + \alpha_0 \right) \right] \right) \tag{4}$$

where α_0 is specified in radians. We set the top of the troposphere at altitude h = 12 km and R_E = 6378 km. This gives S = 360–590 km for α_0 in the range 1–3 degrees. A non-zero index gradient will slightly curve the rays and increase the effective earth radius given by Eq. (A.6). This extends the DX path length as depicted in Fig. 4.

A first-principles analysis of tropospheric scattering was proposed in a seminal paper by Booker and Gordon in 1950 [13]. This widely cited work has stood the test of time with only minor modifications in the past seven decades [14]. For a horizontally polarized radio wave of wavelength λ, the power scattered from an ensemble of turbulent blobs of size L in a volume V is estimated as [15]:

$$\frac{P_S}{P_0} = \kappa \left[\frac{\overline{\Delta n}}{n} \right]^2 \frac{(L/\lambda)^3 \, V\Omega}{\lambda \left[1 + \left(\frac{2L}{\lambda} \sin \frac{\Theta}{2} \right)^2 \right]^2} \tag{5}$$

where P_0 and P_S are the incident and scattered power, respectively, the first bracketed term is the mean-square fractional deviation of the index, and κ is a constant. The scattering volume V may contain multiple pockets of turbulence so that in general $V > L^3$. Overall efficiency is characterized by the solid angle Ω which depends on the antenna aperture, beam divergence, and propagation distance. We take Ω and V as fixed parameters in the following analysis.

The characteristic size of a disturbance relative to the radio wavelength affects the scattering. Normalized scattering power is plotted in Fig. 11 for several ratios L/λ. For a given amount of turbulence, forward scattering is more efficient when the blobs are much larger than a wavelength but also exhibits a strong angular dependence. Backward scattering as is required for weather radar applications generally produces weaker signals.

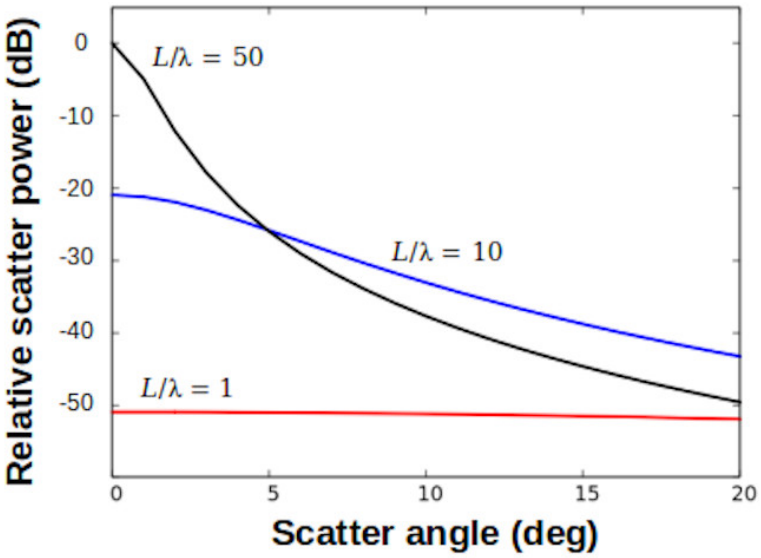

Figure 11: Calculated efficiency of forward scattering in the troposphere as a function of scatter angle Θ. The three curves are for different ratios of the scattering structure size (L) to radio wavelength (λ); curves are normalized to zero angle scattering at $L/\lambda = 50$.

Forward scattering at low altitudes provides an alternative explanation to the perceived phenomenon of ducting. It removes the need for near-horizontal antenna takeoff angles. A significant portion of the radiated RF power will be redirected along the desired trajectory parallel to the surface. This can be more efficient than in usual tropo-scatter geometry where a larger scatter angle Θ is required to direct the signal back to the surface. To illustrate, refer to the curve for

$L/\lambda = 50$ in Fig. 11. Neglect the curvature of the earth and assume transmitting and receiving antennas with takeoff angles of 5 degrees, corresponding to a scatter angle of 10 degrees. The path will have a relative scatter power of about -38 dB. Power from the same transmitter takeoff angle when scattered horizontally, however, will be more than 10 dB stronger. The chordal scatter trajectory is at the desired angle for: i) reflection from an inversion layer or ii) propagating to and scattering from a second volume of turbulence along the weather front, located in proximity to a distant receiving station.

Compared to tropo-scattering at high altitudes, denser air closer to the ground will increase the scattering efficiency due to the multiplying term with Δn in Eq. (5) [14]. In particular, the collision of different temperature air masses that occurs at an inversion will produce vortexes consisting of a mixture of warm and cool air pockets. This results in a strong increase in the average value of Δn and thus scattered power since index variation primarily depends on temperature. The concept is sketched in Fig. 12. Low altitude tropo-scattering represents a more plausible physical model of propagation compared to weak reflections at grazing angles from a well-behaved, stable, mathematically smooth thermal boundary. Turbulent air pockets can be reasonably expected along the length of a warm-cool weather front.

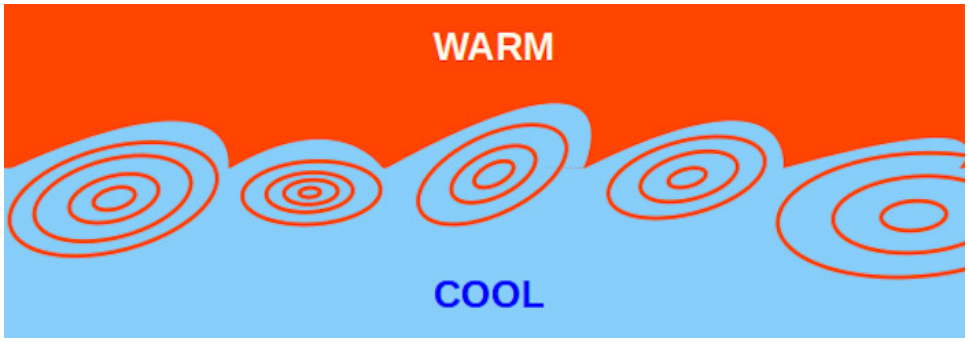

Figure 12: Conceptual illustration of the collision of stratified warm and cool air layers. Vortexes of mixed temperature air form at the interface to produce scattering sites.

If we assume the turbulent thermal boundary follows the curvature of the earth at a constant but relatively low altitude, secondary scattering and/or reflections are needed to attain the observed DX paths of thousands of kilometers. This is shown in Fig. 13. A radio wave is launched from the surface of the earth at angle α_0 and encounters a turbulent interface at altitude h depicted by the dashed blue curve. The segment $S_0 = S/2$, as given by Eq. (4). The wave is then forward-scattered at an angle γ. Secondary scattering is possible when γ is in the range:

$$\sin^{-1}\left[\frac{R_E}{R_E + h}\right] < \gamma < \frac{\pi}{2} \tag{6}$$

as these rays have trajectories above the earth's surface. We emphasize that scattering has the highest efficiency in this range. The segment length $S_1 = (\pi - 2\gamma)R_E$ where γ is measured in radians. For simplicity, scattering back to the earth is also at an angle α_0 [16]. We take $\alpha_0 = 3$ degrees and $h = 2000$ meters, which places γ in the range 88.6–90 degrees with a corresponding maximum distance $2S_0 + S_1 = 392$ km. Adding a third scatter point downrange extends the DX path to 711 km. This picture is consistent with the observation of "leaky ducts" since turbulent protrusions can be expected randomly along the thermal boundary.

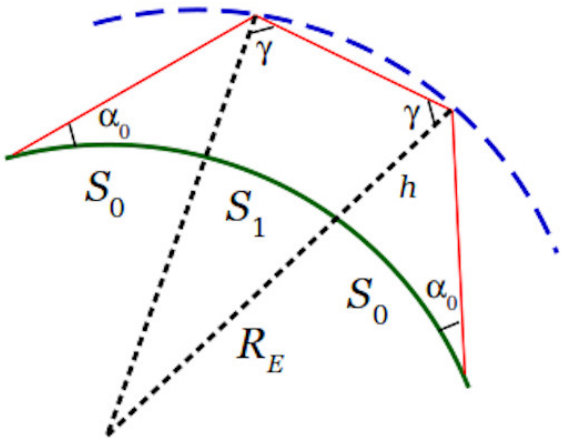

Figure 13: Geometry for analyzing chordal scattering in the troposphere. The turbulent thermal boundary (dashed blue line) follows the earth curvature at an altitude h. Angles and distances are exaggerated for clarity.

Forward scattering described by Eq. (5) has an inverse wavelength dependence and also explains the greater likelihood of observing what is interpreted as ducting at UHF and microwave frequencies. Signals are limited, however, by increased absorption path loss at higher frequencies and we note that the wavelength dependence vanishes for $L \gg \lambda$.

A combination of atmospheric scattering and water reflection may be occurring for the extreme distances that are achieved over the ocean. The seawater surface is well known to act like a metallic reflector at radio frequencies [17]. Assuming a turbulent warm-cool interface at an altitude of 2000 meters and horizontal antenna takeoff angles, the California-Hawaii path could be covered in about 12 hops. This is in contrast to the presently accepted picture of a narrow, elevated duct that requires approximately 40 hops inside an almost perfectly formed air channel. Reflection from the ocean eliminates the restriction of grazing incidence angles at smooth, parallel air boundaries that must remain undisturbed for the duration of the opening.

Conclusion

Ducting in the troposphere has been analyzed using established principles of physical optics: ray tracing, Snell's Law, and Fresnel reflection. Models have been presented for: i) vertical and radial refractive index gradients and ii) abrupt boundary layers. In all cases, the minuscule variation of the refractive index of air severely limits the effectiveness of ray trapping by these mechanisms. While propagation enhancement can occur, it is ineffective for establishing communication paths between two widely separated, ground-based VHF+ stations with non-horizontal antenna takeoff angles. Inversion layers associated with some weather patterns may generate turbulent mixtures of warm and cool air. Sufficiently large and dense vortexes can serve as sites for forward scattering and may explain the enhanced propagation.

References

[1] R.J. Doviak and D.S. Zrnic, *Doppler Radar and Weather Observations*, 2nd ed., Dover Publications (2006).

[2] R.E. Rinehart, *Radar for Meterologists*, 4th ed., Rinehart Publications (2010).

[3] J.C. Schelleng, C.R. Burrows, and E.B. Ferrell, "Ultra-Short-Wave Propagation", Proc. IRE **21**, 427 (1933).

[4] W.I. Orr, *Radio Handbook*, 22nd ed., Indianapolis: Howard Sams (1981).

[5] ARRL News "New World Distance Records Set on 2.3 and 3.4 GHz Ham Bands" June 23, 2015 [Online]. Available: http://www.arrl.org/news/new-world-distance-records-set-on-2-3-and-3-4-ghz-ham-bands.

[6] E. Peacock, "UHF and Microwave Propagation" in *The ARRL UHF/Microwave Experimenter's Manual*, 2nd ed., ARRL Inc. (1990).

[7] M. Born and E. Wolf, *Principles of Optics*, 6th ed., Oxford: Pergamon Press (1980).

[8] Y. Zeng, U. Blahak, M. Neuper, and D. Jerger, "Radar Beam Tracing Methods Based on Atmospheric Refractive Index", J. Atmospheric and Ocean Technology **31**, 2650 (2014).

[9] M.A. Askelson, C.J. Theisen, and R.S. Johnson, "Practical Considerations with Radar Data Height and Great Circle Distance Determination", J. Atmospheric and Ocean Technology **38**, 349 (2021).

[10] H.T. Friis, A.B. Crawford, and D.C. Hogg, "A Reflection Theory for Propagation Beyond the Horizon", Bell System Tech. J. **3**, 627 (1957).

[11] C.G. Purves, "Geophysical Aspects of Atmospheric Refraction", NRL Report 7725 (1974).

[12] Analysis of ray propagation through concentric spherical layers of varying index requires a complicated numerical procedure. Those equations have been omitted here for brevity.

[13] H.G. Booker and W.E. Gordon, "A Theory of Radio Scattering in the Troposphere", Proc. IRE **38**, 401 (1950).

[14] K.S. Gage and B.B. Balsey, "On the scattering and reflection mechanisms contributing to clear air radar echoes from the troposphere, stratosphere, and mesophere", Radio Sci. **15**, 243 (1980).

[15] W.E. Gordon, "Radio Scattering in the Troposphere", Proc. IRE **43**, 23 (1955).

[16] This is essentially the same chordal geometry used to analyze trans-equatorial propagation, although that involves ionospheric physics and much larger distances.

[17] L.K. Lepley and W.M. Adams, "Reflectivity of Electromagnetic Waves at an Air-Water Interface for Pure and Sea Water", WRRCTR Technical Report 25 (1968).

Updates to this document will be posted at: www.sportscliche.com/wb2fko/tech.html.

Appendix A

The radius of curvature r of a ray propagating in the troposphere parallel to the earth's surface is calculated referring to Fig. 14. The ray follows a curved path:

$$S = \beta r = \beta(R_E + h) \tag{A.1}$$

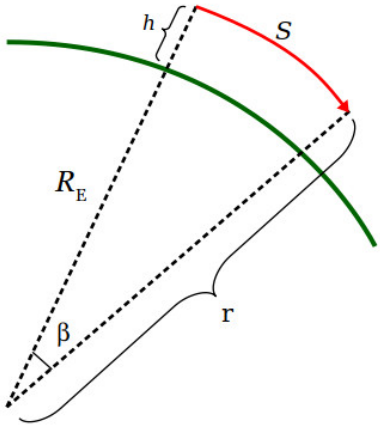

Figure 14: Ray propagating in a curved path S at a height h above the surface of the earth with radius R_E.

This path is covered in time Δt with a velocity v that depends on altitude:

$$S = v(h)\Delta t = \frac{c}{n(h)}\Delta t \tag{A.2}$$

where c is the speed of light and $n(h)$ is the index of refraction. Differentiating with respect to altitude h gives:

$$-\frac{c}{n^2}\frac{dn}{dh}\Delta t = \beta \tag{A.3}$$

Further simplification leads to [8]:

$$\frac{1}{r} = \frac{1}{R_E + h} = -\frac{1}{n(h)}\frac{dn}{dh} \tag{A.4}$$

Using Eqs. (2) and (A.4) with $n_0 = 1.00035$ at $h = 0$ and $R_E = 6378$ km, we find the index gradient required for super-refraction at and parallel to the earth's surface: $\gamma = dn/dh = -156.8 \times 10^{-6}$ km^{-1}.

This model can also be used to calculate the maximum line-of-sight path to the horizon. With an antenna located at height h_A and S measured along the surface we have:

$$S(h = 0) = R_E \left[\frac{\pi}{2} - \sin^{-1}\left(\frac{R_E}{R_E + h_A}\right)\right] \tag{A.5}$$

This assumes no refraction or obstructions. The existence of an index gradient lets us define an effective earth radius [2]:

$$\frac{1}{R'_E} = \frac{1}{R_E} + \frac{dn}{dh}. \tag{A.6}$$

The value of $dn/dh = -39 \times 10^{-6}$ km^{-1} for standard atmospheric conditions leads to the approximation $R'_E \approx (4/3)R_E$. The effective earth radius modifies the line-of-sight distance to the horizon as shown in the following curves generated using Eqs. (A.5) and (A.6). In all conditions, increasing the antenna height gives the expected increase in range.

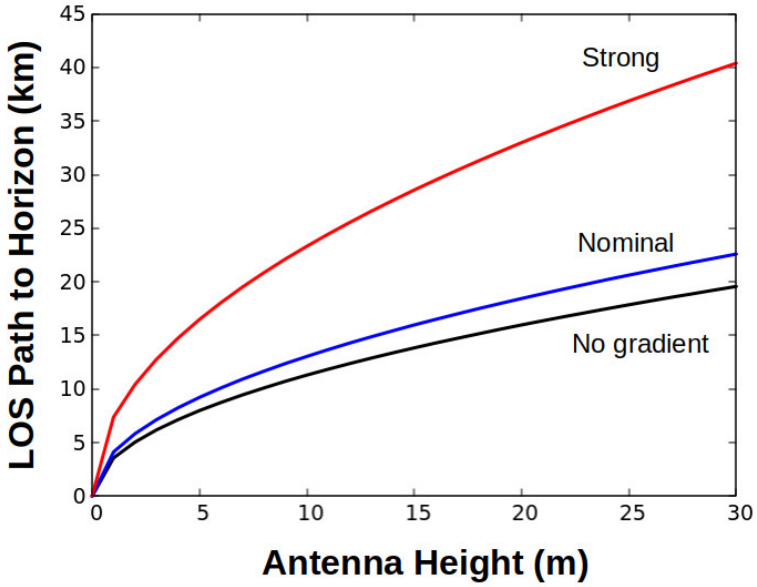

Figure 15: Line-of-Sight distance to the horizon as a function of antenna height for three different refractive index gradients. No gradient (black); Normal conditions with -39×10^{-6} km^{-1} (blue); Strong gradient of -120×10^{-6} km^{-1} (red).

Appendix B

Refraction by planar layers. Referring to Fig. 2, we can re-write Eq. (1) as:

$$n_1 \cos\left(\frac{\pi}{2} - \theta_1\right) = n_2 \cos\left(\frac{\pi}{2} - \theta_2\right). \tag{B.1}$$

Consider vertically stratified layers of differing refractive indices shown in Fig. 16. Sequential application of Snell's Law gives:

$$n_1 \cos\alpha_1 = n_2 \cos\alpha_2 = n_3 \cos\alpha_3 = \ldots = n_m \cos\alpha_m \tag{B.2}$$

which simplifies to:

$$n_1 \cos \alpha_1 = n_m \cos \alpha_m. \tag{B.3}$$

Any refraction taking place in the intermediate layers does not affect the final trajectory, which only depends on the indices of the entrance and exit layers. The ray can propagate through an arbitrary number of refracting layers, but Snell's Law will always limit the exit angle $\alpha_m \geq 0$ degrees, no matter how many layers exist. When the troposphere is modeled as stacked planar layers as shown in Fig. 16, no amount of refraction can return a radio wave launched on the earth's surface back to the surface. This holds true even if the refractive index changes on a continuum and individual layers cannot be distinguished.

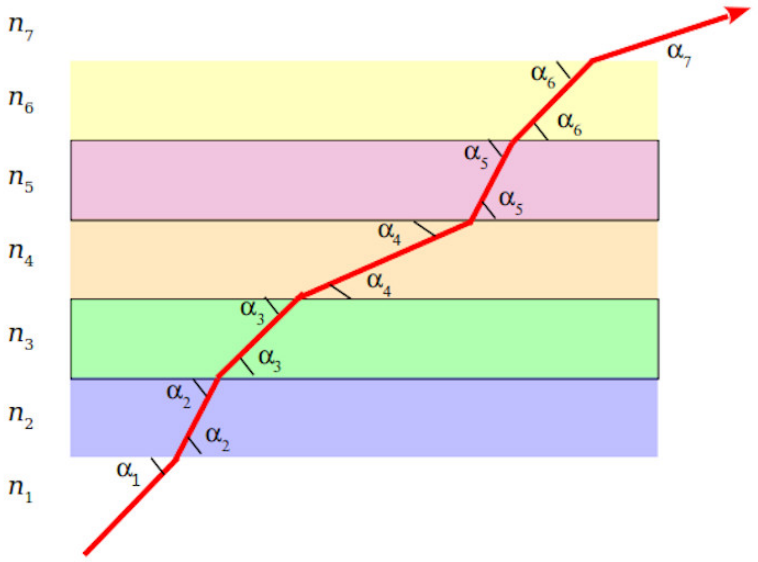

Figure 16: Refraction characterized by Snell's Law in vertical planar layers.

Total internal reflection, however, exists when $\cos \alpha_m = 1$. This will occur if the ray is launched at angle α_0 in a layer with index n_0 and eventually encounters a refractive index n_m that causes the condition:

$$\frac{n_0}{n_m} \cos \alpha_0 \geq 1 \tag{B.4}$$

It is important to emphasize that total internal reflection is not the same as refraction; the concepts are often confused. Equation (B.4) is the key to explaining propagation of light in an optical fiber.

In nominal conditions, the refractive index in the atmosphere decreases linearly with altitude as described by Eq. (2). Ignoring the earth's curvature, total internal reflection occurs at height:

$$h_m = \frac{n_0}{\gamma}(\cos \alpha_0 - 1). \tag{B.5}$$

The reflected ray strikes the surface at a distance S from the transmitter:

$$S = \frac{h_m}{\tan \alpha_0} = \frac{n_0}{\gamma} \frac{\cos \alpha_0 - 1}{\tan \alpha_0} \tag{B.6}$$

Refraction by spherical layers. A realistic model of the troposphere must, of course, consider the curvature of the earth and the analysis becomes more complicated. We follow the approach of Zeng *et al* shown in Fig. 17, where the troposphere is modeled as discrete, concentric layers having the same curvature as the earth [8]. An equivalent analysis can be found in the text by Doviak and Zrnic [1].

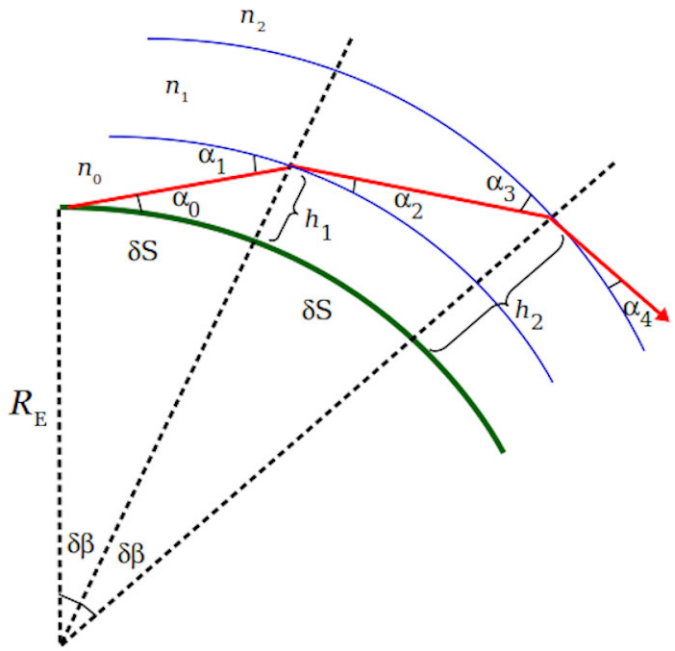

Figure 17: Modeling the troposphere as discrete concentric shells of differing refractive index. The green line is the earth's surface with radius R_E.

A ray is launched at angle α_0 relative to the surface tangent and travels through air with index that varies as a function of altitude $n(h)$. The ray propagates relative to the surface by an incremental amount δS with radial angle $\delta\beta$. At height h_1 the ray encounters a second layer with index $n(h_1)$. The surface normal is defined by the earth radius with an angle of incidence $\pi/2 - \alpha_1$ where $\alpha_1 = \alpha_0 - \delta\beta$. Using Snell's Law:

$$n(0)\cos\alpha_1 = n(0)\cos(\alpha_0 - \delta\beta) = n(h_1)\cos\alpha_2. \tag{B.7}$$

The second interface occurs at height h_2 with the amount of refraction given by:

$$n(h_1)\cos(\alpha_2 - \delta\beta) = n(h_2)\cos\alpha_4. \tag{B.8}$$

Using the Law of Sines applied to the triangle in Fig. 17:

$$\frac{\cos\alpha_2}{R_E + h_2} = \frac{\cos(\alpha_2 - \delta\beta)}{R_E + h_1} = \frac{n(h_2)}{n(h_1)}\frac{\cos\alpha_4}{R_E + h_1} \tag{B.9}$$

where R_E is the radius of the earth. By repeating this procedure and making the appropriate substitutions, the following general relationship is derived for a stack of m spherical layers:

$$n(h_0)\cos\alpha_0 = n(h_m)\frac{R_E + h_m}{R_E + h_0}\cos\alpha_m. \tag{B.10}$$

In the limit $R_E \to \infty$, Eq. (B.3) for planar layers is recovered. This is a general result and is valid for an arbitrary vertical index gradient $n(h)$. As was the case with planar layers, Snell's Law prevents refraction of the ray back to the earth's surface.

Total internal reflection will occur at height h_m when $\cos\alpha_m = 1$. For the specific linear gradient of Eq. (2) applied to Eq. (B.10) with $h_0 = 0$ we get:

$$\cos\alpha_0 = \frac{n(h_m)}{n_0}\frac{R_E + h_m}{R_E} = \frac{(R_E + h_m)(n_0 + \gamma h_m)}{n_0 R_E}. \tag{B.11}$$

This leads to a quadratic equation for h_m:

$$\gamma h_m^2 + (n_0 + \gamma R_E)h_m + n_0 R_E(1 - \cos\alpha_0) = 0 \tag{B.12}$$

with two roots given by:

$$h_m = -\frac{(n_0 + \gamma R_E)}{2\gamma} \pm \frac{1}{2\gamma}\sqrt{(n_0 + \gamma R_E)^2 - 4\gamma n_0 R_E(1 - \cos\alpha_0)} \tag{B.13}$$

Discarding the non-physical root $h_m < 0$, the height h_m is where the ray is completely reflected.

The propagation distance from the source to the reflection point is found using a numerical procedure. The ray path is calculated at small, incremental segments until total reflection occurs at a radial angle $\beta = \sum \delta\beta$ corresponding to a distance along the surface $S = \beta R_E$. The radio wave is reflected back to the surface at a distance $2\beta R_E$ from the transmitter.

Incremental reflectivity at each iteration step is given by the Fresnel formula for a horizontally polarized wave [7]. Referring to Fig. 17:

$$\Gamma_i = \left|\frac{\sin(\alpha_{i+1} - \alpha_i)}{\sin(\pi + \alpha_i + \alpha_{i+1})}\right|^2 \tag{B.14}$$

Internal consistency of the model is verified by comparing the numerical result for height when $\Gamma_i = 1$ to the closed-form analytic solution of Eq. (B.13). The numerical analysis becomes unstable when the wave is launched at or near horizontal due to the extreme grazing angles. Reliable results are obtained for antenna takeoff angles $\alpha_0 > 0.2$ degrees.

Reflection from inversions. Inversion is modeled as two spherical layers having refractive indices n_0 and n_1 with a distinct boundary between them. Referring to Fig. 17, Snell's Law is:

$$n_0\cos\alpha_1 = n_1\cos\alpha_2 \tag{B.15}$$

where

$$\cos\alpha_1 = \frac{R_E}{R_E + h_1} \sin\left(\frac{\pi}{2} + \alpha_0\right). \tag{B.16}$$

In this simple, illustrative model, the ray travels in a straight line to and from the interface where it is partially or completely reflected. Equation (B.14) for the Fresnel reflectivity with horizontal polarization is more conveniently written:

$$\Gamma = \left| \frac{n_0 \sin\alpha_1 - n_1 \sin\alpha_2}{n_0 \sin\alpha_1 + n_1 \sin\alpha_2} \right|^2 \tag{B.17}$$

When the ray is completely reflected ($\Gamma = 1$), it returns to the surface at a distance $2\delta S$ from the source. This distance is given by Eq. (4), recast here using the notation of Fig. 17:

$$2\delta S = 2R_E \left(\frac{\pi}{2} - \alpha_0 - \sin^{-1}\left[\frac{R_E}{R_E + h_1} \sin\left(\frac{\pi}{2} + \alpha_0\right) \right] \right) \tag{B.18}$$